Cancer Biology & Therapy 10:11, 1126-1136; December 1, 2010; © 2010 Landes Bioscience

Inhibition of NADPH oxidase by glucosylceramide confers chemoresistance

Brian M. Barth,[1,2] Sally J. Gustafson,[1] Megan M. Young,[2] Todd E. Fox,[4] Sriram S. Shanmugavelandy,[2] James M. Kaiser,[2] Myles C. Cabot,[3] Mark Kester[2,*] and Thomas B. Kuhn[1]

[1]Program in Biochemistry and Molecular Biology; Department of Chemistry and Biochemistry; University of Alaska-Fairbanks; Fairbanks, AK USA; [2]Department of Pharmacology; [4]Department of Cell and Molecular Physiology; College of Medicine; Pennsylvania State University; Hershey, PA USA; [3]Department of Experimental Therapeutics; John Wayne Cancer Institute at Saint John's Health Center; Santa Monica, CA USA

Key words: NADPH oxidase, chemoresistance, glucosylceramide synthase, antioxidant, glucosylceramide, ceramide, glioblastoma, neuroblastoma, nanoliposome

Abbreviations: 3AT, 3-amino-1,2,4-triazole; DPI, diphenylene iodonium;GCS, glucosylceramide synthase; NOX, NADPH oxidase; PDMP, D-*threo*-1-phenyl-2-decanoylamino-3-morpholino-1-propanol; ROS, reactive oxygen species; TNFα, tumor necrosis factor α

The bioactive sphingolipid ceramide induces oxidative stress by disrupting mitochondrial function and stimulating NADPH oxidase (NOX) activity, both implicated in cell death mechanisms. Many anticancer chemotherapeutics (anthracyclines, Vinca alkaloids, paclitaxel and fenretinide), as well as physiological stimuli such as tumor necrosis factor α (TNFα), stimulate ceramide accumulation and increase oxidative stress in malignant cells. Consequently, ceramide metabolism in malignant cells and, in particular the upregulation of glucosylceramide synthase (GCS), has gained considerable interest in contributing to chemoresistance. We hypothesized that increases in GCS activity and thus glucosylceramide, the product of GCS activity, represents an important resistance mechanism in glioblastoma. In our study, we determined that increased GCS activity effectively blocked reactive oxygen species formation by NOX. We further showed, in both glioblastoma and neuroblastoma cells that glucosylceramide directly interfered with NOX assembly, hence delineating a direct resistance mechanism. Collectively, our findings indicated that pharmacological or molecular targeting of GCS, using non-toxic nanoliposome delivery systems, successfully augmented NOX activity, and improved the efficacy of known chemotherapeutic agents.

Introduction

The primary goal of chemotherapy is to induce cell death in malignant cells. Most chemotherapeutics target various cellular processes associated with survival or growth. Apparently, many chemotherapeutics and endogenous stimuli such as tumor necrosis factor alpha (TNFα) stimulate an accumulation of the sphingolipid ceramide, increase oxidative stress and stimulate apoptosis of tumor cells.[1-3] Sphingolipids are important membrane components and key mediators of cellular signaling, growth and survival, as well as cell death. In particular, ceramide is implicated as a principal mediator of cellular stress pathways, oxidative stress and cellular death mechanisms.[1,2,4-6] Many physiological stimuli, as well as chemotherapeutics, stimulate ceramide accumulation through various mechanisms such as stimulation of de novo synthesis, degradation of complex sphingolipids or inhibition of ceramide catabolism.[2,3,7] The NADPH oxidase (NOX) is an oxidoreductase that can rapidly produce reactive oxygen species (ROS), and has been shown to be stimulated by ceramide.[5] NOX enzymes are multi-subunit complexes of both membrane-bound and cytsolic subunits. For most NOX isoforms, assembly of these subunits is critical to the functional activation of the enzyme.[4,8,9]

NOX enzymes play key roles in the regulation of cellular processes, including growth and proliferation.[4] In particular, NOX enzymes have been shown to regulate phosphatases and transcription factors, often via redox-sensitive cysteine residues, thereby influencing receptor-initiated signaling cascades.[4] Studies have demonstrated elevated NOX1 or NOX4 expression in cancers of the breast[10] and colon,[11] as well as leukemia.[12] In contrast, NOX enzymes have also been shown to restrict the maturation and proliferation of B cells,[13] as well as to induce cell death in a wide variety of cell and tissue types.[4]

Multidrug resistance poses a major problem in the treatment of cancer. Some types of cancer are intrinsically resistant, as is the case with some glioblastomas,[14,15] while other types of cancer cells can acquire resistance during the course of treatment or relapse with resistance, to the chemotherapeutic(s) used during treatment.[16] Ceramide metabolism in malignant cells has gained considerable interest as a key contributor to chemoresistance. In particular, the upregulation of glucosylceramide synthase (GCS) has been implicated as a major chemoresistance mechanism

*Correspondence to: Mark Kester; Email: mkester@psu.edu
Submitted: 08/19/10; Accepted: 08/28/10
DOI: 10.4161/cbt.10.11.13438

by neutralzing ceramide through a conversion to glucosylceramide.[7,16,17] Intriguingly, a genetic deficiency in cerebrosidase termed Gaucher disease (type I), results in the accumulation of glucosylceramide, as it is unable to be degraded.[18] A phenotype of this cerebrosidase deficiency, monocyte dysfunction, is strikingly similar to that of chronic granulomatous disease, a genetic deficiency in one or more of NOX subunits.[4,18]

In this study, the role of GCS in conferring chemoresistance was further investigated with a focus on NOX and implications on oxidative stress. Previously, we had demonstrated that TNFα, a known stimulator of ceramide, elicited oxidative stress by upregulating NOX activity in SH-SY5Y neuroblastoma cells.[19] Similarly, many chemotherapeutics have been shown to induce oxidative stress.[20,21] We therefore hypothesized that increased glucosylceramide production through GCS could interfere with NOX activity as a mechanism critical to chemotherapeutic-resistance. Utilizing pharmacological and molecular techniques, we demonstrated that glucosylceramide potently interfered with agonist-stimulated NOX activity. NOX-mediated ROS production was abolished by blocking the functional assembly of cytosolic and membrane subunits of NOX. We further showed in glioblastoma cells that depleting GCS activity not only augmented NOX activity but improved the efficacy of chemotherapy.

Results

Chemotherapeutics stimulate NOX-dependent intracellular ROS production. A series of chemotherapeutic agents were evaluated for their ability to stimulate the production of intracellular ROS in human SH-SY5Y neuroblastoma cells (**Fig. 1**). We utilized the established NOX inhibitor diphenylene iodonium (DPI) to demonstrate a key role for NOX in chemotherapeutic-stimulated ROS production.[4] We found that significant NOX-dependent intracellular ROS production was stimulated in response to the anthracycline doxorubicin (**Fig. 1A**), the mitotic inhibitor paclitaxel (**Fig. 1B**), the estrogen receptor antagonist 4-hydroxy tamoxifen (**Fig. 1C**), the anti-metabolite methotrexate (**Fig. 1D**), the nucleoside analog gemcitabine (**Fig. 1E**) and the retinoid derivative fenretinide (**Fig. 1F**). These results not only implicated known generators of ceramide to the generation of intracellular ROS but also attributed NOX a role as the principal source of ROS. In fact, tamoxifen (an antagonist of P-glycoprotein) leads to an accumulation of ceramide by inhibiting glucosylceramide production and whereas fenretinide increases de novo synthesis of ceramide by stimulating serine palmitoyltransferase.[22,23] Furthermore, fenretinide blocks dihydroceramide desaturase leading to accumulations of dihydroceramide.[22,23]

To further substantiate a ceramide-mediated NOX stimulation, we directly delivered the short chain ceramide analog C6-ceramide using nanoliposomal formulations, which demonstrated in vivo efficacy in rodent models of breast cancer and melanoma.[24,25] Furthermore, the C6-ceramide nanoliposomal formulation has been extensively characterized by the Nanotechnology Characterization Laboratory of the National Cancer Institute and most importantly was shown to be free of toxic side effects associated with other anti-neoplastic agents.[26] The ghost formulation was a control formulation that did not contain any ceramide and, as expected, did not stimulate the production of intracellular ROS (**Fig. 1G**). Comparatively, we observed significant NOX-dependent production of intracellular ROS in response to treatment with the C6-ceramide formulation (**Fig. 1H**). Moreover, 40% greater ROS production was achieved when using a nanoliposomal formulation which contained D-*threo*-1-phenyl-2-decanoylamino-3-morpholino-1-propanol (PDMP), an inhibitor of GCS (the enzyme that converts ceramide to glucosylceramide), in addition to C6-ceramide (**Fig. 1I**).[16,17] This later finding demonstrated that blocking GCS dramatically improved the efficacy of nanoliposomal C6-ceramide-stimulated NOX-dependent intracellular ROS production in neuroblastoma cells.

Glioblastoma cells exhibit elevated antioxidant capacity compared to neuroblastoma cells. In addition to research identifying increased ceramide metabolism in chemoresistant cancers, reports have emerged documenting increased antioxidant defenses in radio- and chemoresistant glioblastomas.[15] In our study, we compared the activities of catalase and superoxide dismutase, primary antioxidant enzymes, and the activity of GCS in human SH-SY5Y neuroblastoma cells, human U-87 MG glioblastoma cells and human LN-18 glioblastoma cells (**Fig. 2A**). We found that the activities of all these enzymes were significantly greater in either glioblastomas compared to activities measured in the neuroblastoma cell line. In context with these findings, we also found that SH-SY5Y neuroblastoma cells responded to doxorubicin with a robust increase in intracellular ROS production, whereas U-87 MG and LN-18 glioblastoma cells did not (**Fig. 2B**).

Glucosylceramide blocks agonist-stimulated NOX activity. The neutralization of ceramide by elevated GCS activity is accepted as the role for GCS in therapy-resistant cancer. However, no specific role for the product of GCS activity, glucosylceramide, has been described. We investigated whether agonist-stimulated NOX activity could be impeded directly by GCS's production of glucosylceramide. In fact, we found that the addition of exogenous glucosylceramide to SH-SY5Y neuroblastoma cells blocked NOX activation. As an indication of NOX activation, we measured the movement of the cytosolic subunit $p67^{phox}$ to the plasma membrane where it and other cytosolic subunits, complex with membrane-bound subunits to form the active enzyme.[4] We found that glucosylceramide blocked TNFα-stimulated $p67^{phox}$ translocation to the plasma membrane (**Fig. 2C**). This finding was critical because it showed, in a cellular paradigm, that glucosylceramide itself blocked the assembly of NOX. As anticipated, we observed that TNFα-stimulated intracellular ROS production was abrogated by exogenous glucosylceramide (**Fig. 2D**).

Blunting GCS augments intracellular ROS production. We found that pharmacological inhibition of GCS using PDMP augmented doxorubicin-induced intracellular ROS formation in SH-SY5Y neuroblastoma cells, and even restored the effect in U-87 MG and LN-18 glioblastoma cells (**Fig. 3A–C**). We also observed that 3-amino-1,2,4-triazole (3AT), an inhibitor of the antioxidant enzyme catalase, augmented doxorubicin-induced intracellular ROS accumulation in SH-SY5Y neuroblastoma cells and restored doxorubicin effectiveness in U-87 MG and LN-18 glioblastoma cells (**Fig. 3A–C**). Since the use of pharmacological

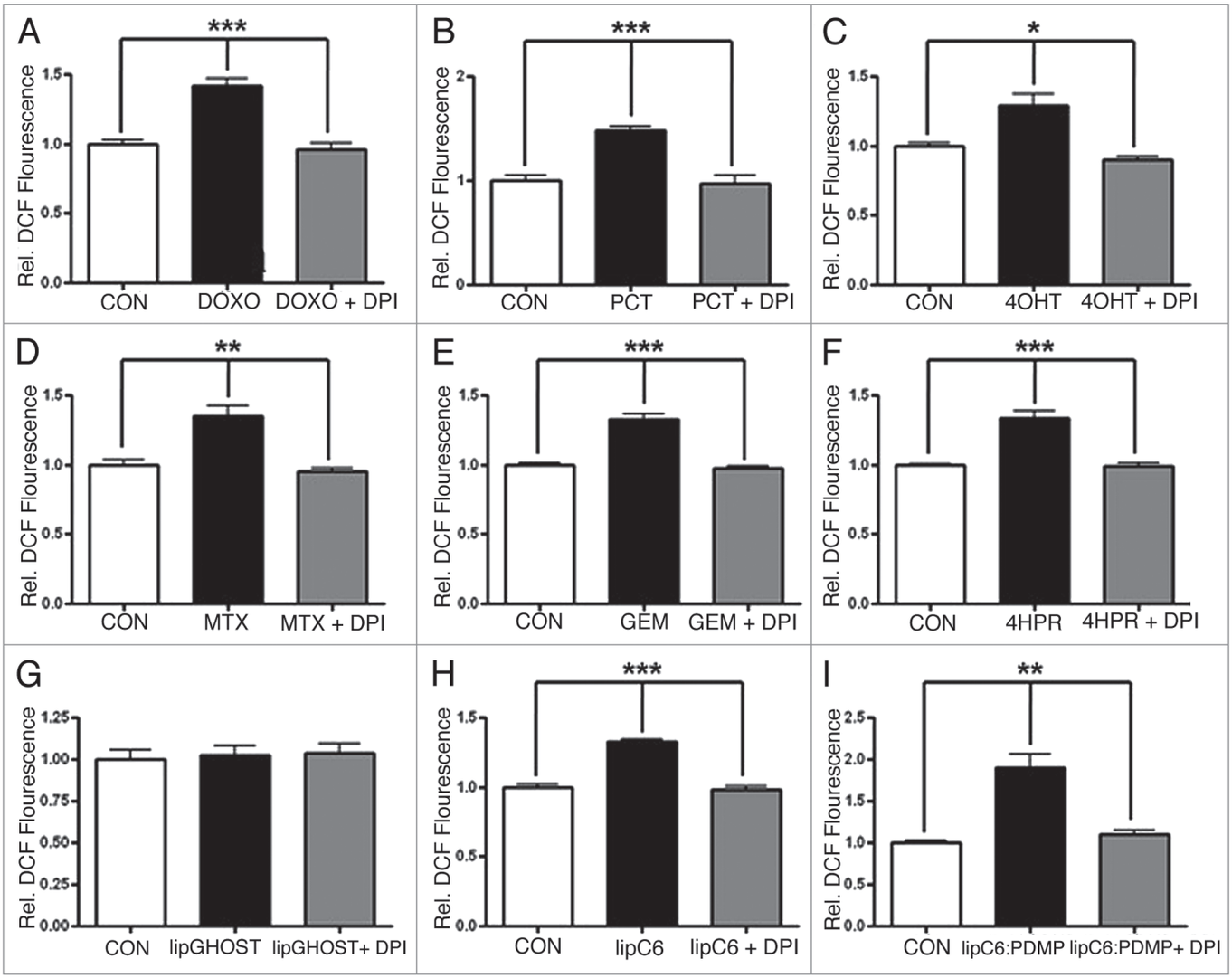

Figure 1. Chemotherapeutics stimulate NOX-dependent intracellular ROS production. The production of intracellular ROS was evaluated using the redox-sensitive indicator H_2DCFDA in human SH-SY5Y neuroblastoma cells. Diphenylene iodonium (DPI, 10 μM, 60 min pretreatment), an inhibitor of NOX, was utilized to demonstrate the NOX-dependence of ROS production in response to various chemotherapeutics. (A) Doxorubicin (DOXO, 8.6 μM, 90 min). (B) Paclitaxel (PCT, 100 nM, 60 min). (C) 4-hydroxy tamoxifen (4OHT, 7.4 μM, 90 min). (D) Methotrexate (MTX, 1 μM, 60 min). (E) Gemcitabine (GEM, 1 μM, 120 min). (F) Fenretinide (4HPR, 1.5 μM, 60 min). (G) Empty (ghost) nanoliposomes (lipGH, 60 min). (H) Nanoliposomes containing 5 μM C6-ceramide (lipC6, 60 min). (I) Nanoliposomes containing both 5 μM C6-ceramide and 5 μM PDMP (lipC6/PDMP, 60 min). Fluorescence, corresponding to ROS, was normalized to the average fluorescence of the control (relative DCF-fluorescence). Data represent the mean ± SEM of four independent experiments; *$p < 0.05$, **$p < 0.01$ or ***$p < 0.001$, as determined by 1-way ANOVA.

agents has drawn some criticism due to issues with solubility, specificity or toxicity, we employed the more direct approach, the molecular targeting of GCS utilizing siRNA.[26] An important aspect of our approach was the use of a non-toxic cationic nanoliposomal delivery method. Typical cationic transfection reagents are impractical for in vivo use due to severe toxicity. However, our laboratory has designed and tested a unique formulation that has shown promise in animal studies, both as an efficacious and non-toxic delivery system.[27-29] In this study, we demonstrated that siRNA directed against GCS significantly augmented doxorubicin-induced intracellular ROS production in SH-SY5Y neuroblastoma cells, while a non-targeted siRNA was ineffective (**Fig. 3A**). Likewise, significant doxorubicin-induced intracellular ROS production was restored in both U-87 MG and LN-18 glioblastoma cells when targeted by siRNA directed against GCS, but not a non-targeted siRNA (**Fig. 3B and C**).

Downregulation of GCS improves chemotherapy-induced cell death. In addition to increasing the production of intracellular ROS, both PDMP and 3AT improved doxorubicin-induced cell death in the neuroblastoma and glioblastoma cell lines (**Fig. 3D and F**). Furthermore, by targeting GCS with specific siRNA, but not non-targeted siRNA, we demonstrated a significant decrease in doxorubicin-mediated cell viability in the neuroblastoma and glioblastoma cell lines (**Fig. 3D and F**). These results showed that targeting GCS, the enzyme responsible for neutralizing ceramide and synthesizing NOX-impeding glucosylceramide, augmented

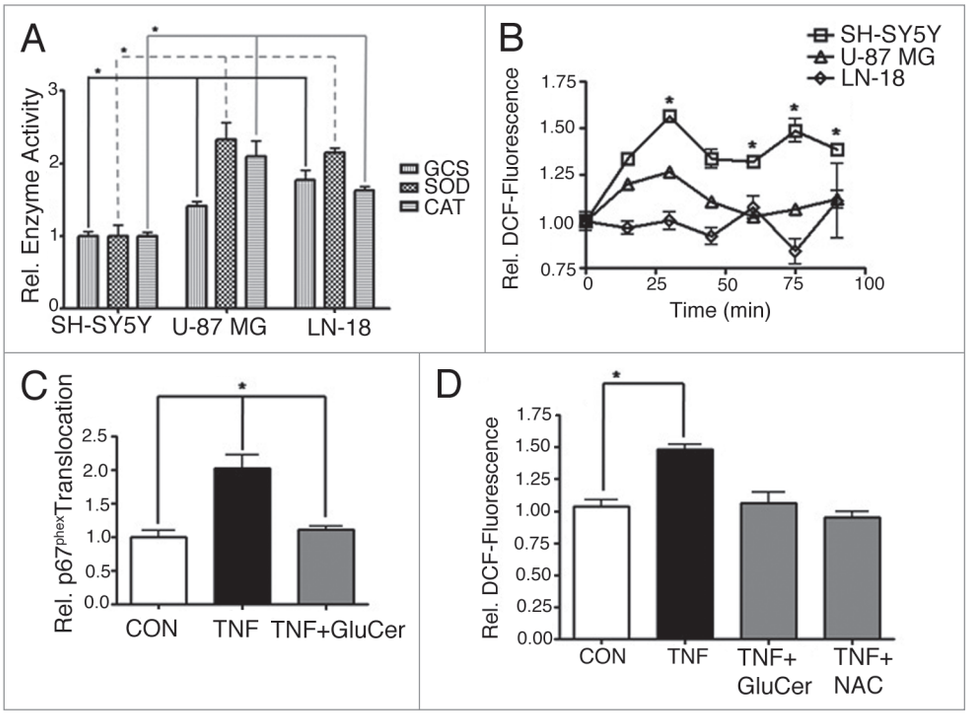

Figure 2. Glucosylceramide blocks agonist-stimulated NOX activity. (A) Basal activities of catalase (CAT), superoxide dismutase (SOD) and glucosylceramide synthase (GCS) were compared between human SH-SY5Y neuroblastoma, U-87 MG glioblastoma and LN-18 glioblastoma cells. Activities were normalized to the average activities of SH-SY5Y cells. Data represent the mean ± SEM of at least three independent experiments; *p < 0.05, as determined by 1-way ANOVA. (B) The redox-sensitive indicator H_2DCFDA was used to compare production of intracellular ROS between SH-SY5Y, U-87 MG or LN-18 cells in response to doxorubicin (8.6 μM). Fluorescence, corresponding to ROS, was normalized to the average 0-min fluorescence of the respective cell line (relative DCF-fluorescence). Data represent the mean ± SEM of three independent experiments; *p < 0.05, as determined by 2-way ANOVA, comparing SH-SY5Y response to both U-87 MG and LN-18 response. (C) Translocation of $p67^{phox}$ to the plasma membrane was evaluated as an indication of NOX assembly. SH-SY5Y cells were exposed to TNFα (TNF, 100 ng/ml, 15 min) ±60 min pretreatment with exogenous C8-glucosylceramide (GluCer, 10 μM). Translocation was normalized to the average translocation of the control. Data represent the mean ± SEM of three independent experiments; *p < 0.01, as determined by 1-way ANOVA. (D) Intracellular ROS production was evaluated in SH-SY5Y cells exposed to TNFα (TNF, 100 ng/ml, 60 min) ±60 min pretreatment with GluCer (10 μM) or the antioxidant N-acetyl-L-cysteine (NAC, 5 mM). Data represent the mean ± SEM of three independent experiments; *p < 0.01, as determined by 1-way ANOVA.

chemotherapy-stimulated intracellular ROS production and cell death.

Overexpression of GCS blocks NOX-mediated ROS production and improves cell survival. Overall, our studies revealed that the SH-SY5Y neuroblastoma cell line was responsive to agonist-stimulated NOX activity, compared to the U-87 MG and LN-18 glioblastoma cell lines tested. Since blunting GCS activity augmented both doxorubicin-induced NOX activity and neuroblastoma cell death, we opted to overexpress GCS as a means to further verify its role in chemoresistance. Transfection of SH-SY5Y neuroblastoma cells with a plasmid encoding FLAG-tagged GCS completely blocked both TNFα- stimulated intracellular ROS production (**Fig. 4A**) and doxorubicin-stimulated intracellular ROS production (**Fig. 4B**). Furthermore, overexpression of GCS completely blocked TNFα-stimulated SH-SY5Y cell viability loss (**Fig. 4C**) and also very modestly, yet significantly, blocked doxorubicin-stimulated SH-SY5Y cell viability loss (**Fig. 4D**). Lastly, we demonstrated that overexpression of GCS specifically interfered with TNFα-stimulated assembly of NOX in neuroblastoma cells, indicated as an absence of $p67^{phox}$ translocation to the plasma membrane. In sharp contrast, siRNA directed against GCS, but not non-targeted siRNA, augmented TNFα-stimulated $p67^{phox}$ translocation (**Fig. 4E**).

Glucosylceramide alters membrane curvature. While manipulating GCS by various methods offered the perspective that ceramide neutralization impeded NOX, exogenous glucosylceramide-driven impediment of NOX was not explained. Important to understanding this phenomenon is the fact that while GCS resides on the cytosolic leaflet of the Golgi apparatus, glucosylceramide is promptly re-located to the luminal side.[30] For this reason, natural glucosylceramide is found predominantly on the extracellular leaflet of the plasma membrane, the same location as exogenously added glucosylceramide. Furthermoe, glucosylceramide has essentially no lateral diffusion within the plasma membrane due to the hydrophilicty of its head group.[30] Therefore, we speculated that glucosylceramide interfered with NOX assembly via a biophysical mechanism. By studying liposome models of the plasma membranes, we observed that the addition of glucosylceramide significantly decreased the size of these vesicles (**Fig. 5A**). The size of a vesicle is a measure of curvature (equal to the reciprocal of the radius), in that a smaller vesicle

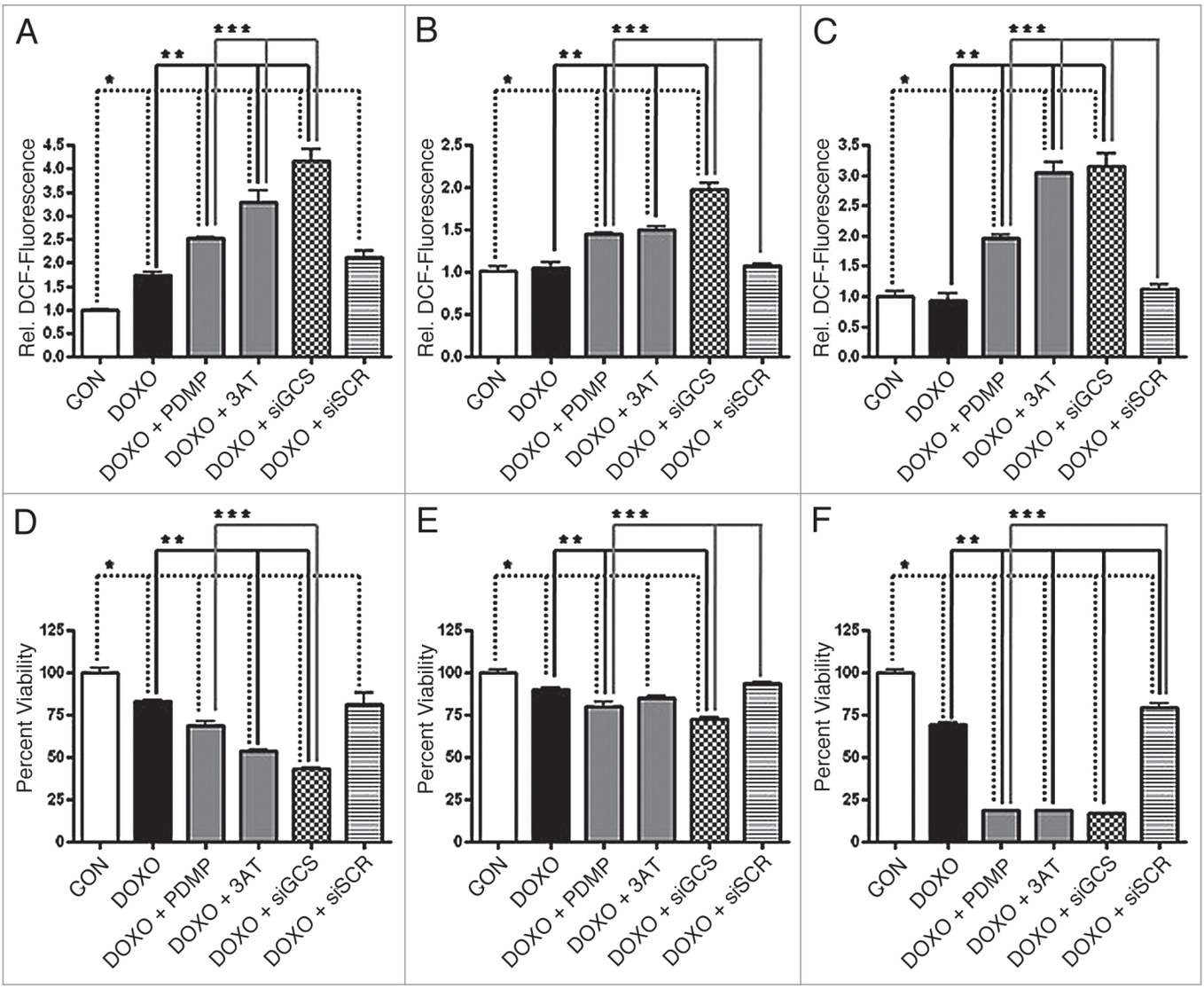

Figure 3. Interference with GCS augments intracellular ROS production and improves chemotherapy-induced cell death. Cells were exposed to doxorubicin (DOXO, 8.6 μM) ±2 h pretreatment with the GCS inhibitor PDMP (10 μM) or the catalase inhibitor 3-amino-1,2,4-triazole (3AT, 1 mM). Alternatively, cells were transfected with 200 nM siRNA directed against GCS (siGCS) or non-targeted siRNA (siSCR), 48 hours prior to treatment. The production of intracellular ROS was examined after 90 min treatment in human SH-SY5Y neuroblastoma, U-87 MG glioblastoma or LN-18 glioblastoma cells, using the redox-sensitive indicator H_2DCFDA, while cellular viability was determined after 48 hour treatment by XTT assay. Fluorescence, corresponding to ROS, was normalized to the average fluorescence of the control (relative DCF-fluorescence). (A) ROS in SH-SY5Y cells. (B) ROS in U-87 MG cells. (C) ROS in LN-18 cells. (D) Viability of SH-SY5Y cells. (E) Viability of U-87 MG cells. (F) Viability of LN-18 cells. Data represent the mean ± SEM of four independent experiments; *$p < 0.05$ compared to control (CON), **$p < 0.05$ compared to DOXO, ***$p < 0.05$ compared to DOXO + PDMP, as determined by 1-way ANOVA.

is more curved. Therefore, we postulated that glucosylceramide interferes with NOX by perturbing the membrane, inducing positive curvature, which restricts subunit-subunit and subunit-membrane interactions (**Fig. 5B**).

Discussion

Only recently have functional NOX (NOX1-5) activities, similar to the well-documented NOX2 in phagocytes, been identified in many non-phagocytic cell types (microglia, astrocytes, neurons) as a source of ROS production in response to stimuli such as TNFα.[4] Importantly, several lipids including arachidonic acid and anionic phospholipids are critical in the activation mechanism of NOX enzymes.[4,31] A recent study also demonstrated that ceramide synthesized de novo from the saturated fatty acid palmitate, induced the activation of NOX in retinal pericytes.[5] Many chemotherapeutics, as well as endogenous stimuli such as TNFα, stimulate ceramide accumulation and induce apoptosis in tumor cells.[2,32,33] Mechanisms of chemoresistance have therefore developed to evade the toxic effects of ceramide, by neutralization, degradation or conversion to pro-mitogenic and pro-survival metabolites.[2] Moreover,

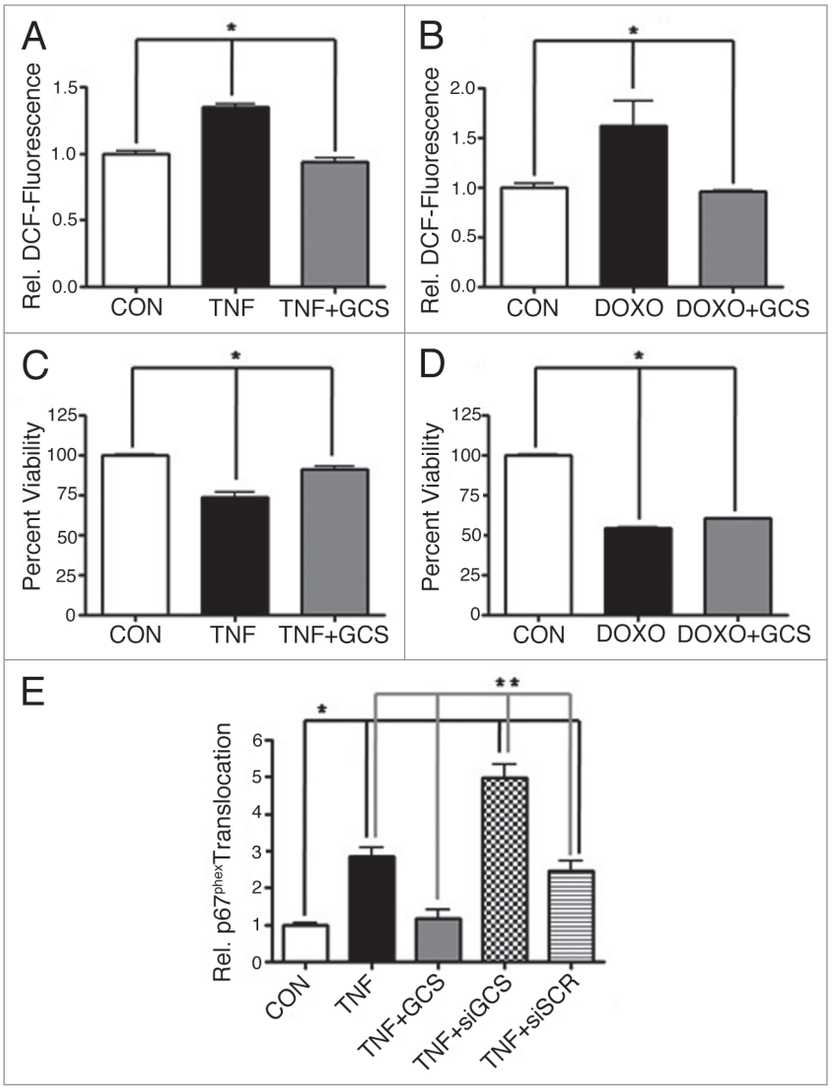

Figure 4. Overexpression of GCS blocks NOX and improves survival. Human SH-SY5Y neuroblastoma cells were transfected with 3 μg/ml of a GCS-expressing plasmid, 200 nM siRNA directed against GCS (siGCS) or non-targeted siRNA (siSCR), 48 hours prior to treatment. The production of intracellular ROS was evaluated using the redox-sensitive indicator H_2DCFDA, while cellular viability was determined by XTT assay. Fluorescence, corresponding to ROS, was normalized to the average fluorescence of the control (relative DCF-fluorescence). (A) ROS in cells exposed to TNFα (TNF, 100 ng/ml, 60 min). (B) ROS in cells exposed to doxorubicin (DOXO, 8.6 μM, 90 min). (C) Viability of cells exposed to TNFα (TNF, 100 ng/ml, 48 h). (D) Viability of cells exposed to doxorubicin (DOXO, 8.6 μM, 48 h). Data represent the mean ± SEM of four (viability) or five (ROS), independent experiments; *$p < 0.05$, as determined by 1-way ANOVA. (E) Translocation of $p67^{phox}$ to the plasma membrane was evaluated as an indication of NOX assembly. Translocation was normalized to the average translocation of the control and represent the mean ± SEM of three independent experiments; *$p < 0.05$ compared to control (CON), **$p < 0.01$ compared to TNF + siGCS, as determined by 1-way ANOVA.

oxidative stress resistance of tumor cells has also recently been described in the form of increased catalase activity in rat glioblastoma cells.[15] Therefore, it became important to evaluate the role of chemoresistant pathways that metabolize ceramide, such as GCS, in the regulation of NOX activity. Intriguingly, glucosylceramide was shown to interfere with NOX in crude cell-free systems.[18,34] In this respect, the phenotype of Gaucher disease (type I), a cerebrosidase deficiency, is strikingly similar to that of the NOX-deficiency chronic granulomatous disease.[4,18] We therefore hypothesized that glucosylceramide could interfere with NOX activity and that this was critical to the chemotherapeutic-resistance mechanism of GCS.

In this study, we observed that various chemotherapeutics stimulated an increase in intracellular ROS production, which was completely blocked by an inhibitor of NOX enzymes (**Fig. 1**). Additionally, liposomal ceramide stimulated NOX-dependent intracellular ROS accumulation as opposed to a liposomal formulation containing no ceramide. More so, addition of the GCS inhibitor, PDMP, to the liposomal ceramide formulation dramatically augmented its ability to stimulate NOX-dependent intracellular ROS accumulation. Altogether, these results strongly indicated that ceramide and generators of ceramide stimulated intracellular production of ROS in SH-SY5Y neuroblastoma cells, which was attributed to NOX enzymes. We next observed

that U-87 MG and LN-18 glioblastoma cells had elevated GCS, catalase and superoxide dismutase activities, consistent with potential mechanisms of multidrug-resistance (**Fig. 2A**). Not surprisingly, these glioblastoma cell lines had a diminished capacity to generate intracellular ROS in response to doxorubicin (**Fig. 2B**). Further investigation showed that pharmacological inhibitors of catalase or GCS or siRNA directed against GCS, restored or augmented the ability of the glioblastoma and neuroblastoma cell lines to produce intracellular ROS in response to doxorubicin (**Fig. 3**). More importantly, this restoration in ROS generation was accompanied by a concomitant decrease in the viability of these cancerous cell lines. In contrast, the overexpression of GCS in the more sensitive neuroblastoma cells rendered them resistant to doxorubicin or TNFα (**Fig. 4A and B**).

These findings demonstrating that targeting of GCS can improve the efficacy of chemotherapy, or that overexpression of GCS can induce resistance, were consistent with the defined multidrug-resistance mechanism of ceramide neutralization by GCS. However, we also observed that addition of exogenous glucosylceramide could block the responsiveness of SH-SY5Y cells to stimuli mediating intracellular ROS production (**Fig. 2C**). Moreover, exogenous glucosylceramide directly interfered with $p67^{phox}$ translocation to the plasma membrane, a critical step in functional NOX assembly (**Fig. 2D**). These findings were corroborated with additional molecular approaches manipulating endogenous glucosylceramide levels such as utilizing siRNA directed against GCS or overexpression of GCS. Depleting GCS activity with siRNA augmented $p67^{phox}$ translocation to the plasma membrane, whereas overexpression of GCS blocked this same translocation (**Fig. 4C**). The ability of exogenous and endogenous glucosylceramide to block NOX assembly was further studied at a biophysical level utilizing model membranes in the form of liposomes. Exogenous glucosylceramide incorporates into the outer leaflet of the plasma membrane, with no lateral diffusion across this membrane. In comparison, endogenous glucosylceramide, which is generated on the cytosolic leaflet of the Golgi, is ultimately relocated to the inner leaflet of the Golgi where it is metabolized into other glycosphingolipids or transported to the outer leaflet of the plasma membrane. It was therefore important to understand how a lipid added to the outer leaflet of the plasma membrane, exogenously or endogenously, could interfere with NOX enzymes localized on the cytosolic leaflet. Using model membrane liposomes, we demonstrated that glucosylceramide induced positive curvature, evidenced by a significant decrease in the size of the liposomes (**Fig. 5A**). We therefore speculated that positive curvature of a membrane may interfere with the assembly of NOX enzymes (**Fig. 5B**). Altogether, our findings demonstrated a novel mechanism whereby glucosylceramide, the product of GCS activity, could interfere with NOX activity by preventing proper assembly of the enzyme.

These findings argue that GCS's role in chemoresistance is more profound than previously thought. While ceramide neutralization by GCS may also result in NOX inactivity, as ceramide stimulates NOX, the ability of exogenous glucosylceramide to block NOX activity clearly demonstrates a distinct inhibitory mechanism. Another important aspect of this study is the link of NOX enzymes to the efficacy of chemotherapy. In contrast, antioxidant therapy is a well recognized preventative and therapeutic approach to cancer. In addition, a recent study specifically defined NOX4 as a possible oncoprotein.[10] Importantly, NOX4's localization to the mitochondria was evaluated and suggested to be important to the transformation of cells. In reconciling the differences with this NOX4 study, it is important to note that NOX4 is considered to be a constitutively active enzyme with no requirement for cytosolic cofactors to assemble with membrane-bound subunits.[4,8] In contrast to the NOX4 study, we have showed in previous studies,[19] as well as the current study, that agonist-dependent stimulation of NOX-dependent activity involves cytosolic cofactors translocating to the plasma membrane. More so, in the current study, interference of agonist-stimulated NOX assembly by exogenously-delivered glucosylceramide critically depended on the presence of the enzyme at the plasma membrane. Overall, our findings are specific to a chemotherapy-responsive NOX enzyme that is distinct from the potential cancer-promoting NOX4.

In summary, ceramide neutralization through the formation of glucosylceramide not only decreases the proapoptotic stimulus ceramide but also abolishes NOX assembly and activity (**Fig. 5C**) and in conjunction with increased antioxidant enzyme activities, greatly alleviates cell death-inducing oxidative stress associated with chemotherapy or physiological agonists. Consequently, pharmacological inhibition of antioxidant enzymes, such as catalase or pharmacological or molecular inhibition of GCS restored doxorubicin-toxicity, offering promise as a useful therapeutic avenue for the treatment of advanced cancers of the CNS. While treatment of patients with siRNA is currently not possible due to toxicity associated with delivery systems, our non-toxic cationic nanoliposomal formulation is designed specifically to overcome this hurdle. Additionally, our nanoliposomal formulation combining C6-ceramide and PDMP overcomes the current hurdle to clinical delivery of the GCS inhibitor PDMP associated with its low solubility. Nanoscale delivery systems further offer considerable clinical potential in the delivery of lower, yet more concentrated, therapeutic doses.[26,35] Many advanced CNS tumors, such as glioblastomas, respond poorly to chemotherapeutic and radiation therapies, while in comparison, resistance in neuroblastomas is less common.[14,36] Complicating matters and driving the demand for new and better therapeutics, is the fact that glioblastoma multiform, the most common primary brain tumor, has one of the worst survival rates among all cancers.[14] This research offers an important advance to the understanding of mechanisms of multidrug-resistance in glioblastoma and the design of better therapeutics. On the other hand, it is worth noting that degenerative pathologies, including acute and chronic CNS disorders as well as psychiatric disorders, exhibit oxidative stress as a major component.[37,38] This is important because in contrast to the goals of cancer therapy, the goals in the treatment of degenerative disorders are to improve the survival and function of normal cells. While ceramide neutralization and degradation are hallmarks of chemoresistance, ceramide accumulation is characteristic of degenerative disorders.[6,32,33,38] Altogether, nano-encapsulated

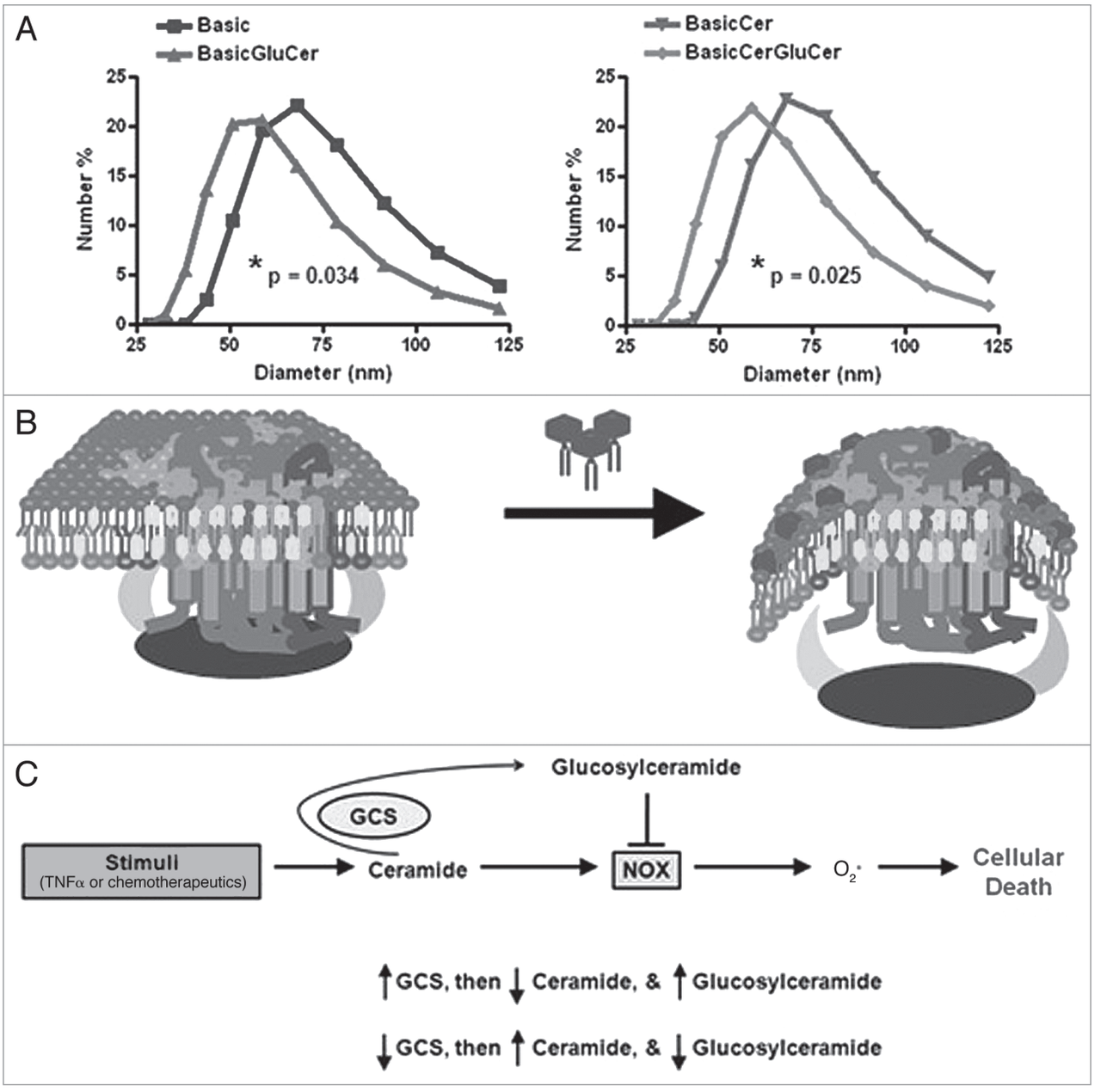

Figure 5: Glucosylceramide prevents NOX activity by altering membrane curvature. Liposomes were prepared as a model of the plasma membrane, and the effect on membrane curvature with glucosylceramide addition was evaluated. (A) Liposomes composed of phospholipids, cholesterol, and sphingomyelin (basic formulation), with or without ceramide, were compared to equivalent counterparts containing glucosylceramide. Size of liposomes, related to curvature (curvature = 1/radius), was determined by light scattering. Data represent the mean of three independent experiments. Significance was determined by unpaired t-test of the mean diameter of respective liposomes. (B) Model depicting the addition of glucosylceramide inducing positive membrane curvature, which restricts the ability of NOX cytosolic components to interact with essential membrane lipids (glucosylceramide: dark hexagons with tails). (C) Schematic depicting that TNFα, or chemotherapeutics, stimulates NOX through ceramide generation, and that neutralization to glucosylceramide directly blocks NOX while also depleting ceramide.

pharmacological or molecular agents targeting GCS offer exceptional promise in the treatment of chemoresistant CNS cancers, based on our findings that downregulating GCS activity not only can override ceramide neutralization by tumor cells, but also reengage stimuli-dependent NOX activity, restoring an ability to produce ROS and ultimately inducing tumor cell death.

Materials and Methods

Reagents. DMEM and penicillin/streptomycin solution were obtained from Mediatech (Herndon, VA). Solutions of GlutaMAX-1 and trypsin/EDTA, Hank's Balanced Salt Solution (HBSS) and Amplex Red reagent, as well as fluorescent siRNA, were from Invitrogen (Carlsbad, CA). Fetal bovine serum was

from Atlanta Biologicals (Atlanta, GA). The ON-TARGET plus SMART pool siRNA directed against GCS and non-targeting siRNA was from Dharmacon (Lafayette, CO). GCS cDNA (Gene: UGCG; Accession: BC038711), was purchased from Thermo Fisher Scientific (Huntsville, AL). Streptavidin-agarose beads, sulfo-NHS-biotin, protease inhibitor cocktail (PIC), a Pico Super Signal chemoluminescent kit and a BCA protein assay kit were obtained from Pierce (Rockland, IL). Polyclonal rabbit anti-GCS, rabbit anti-FLAG, rabbit anti-GAPDH and $p67^{phox}$ antibodies, and corresponding horseradish peroxidase-conjugated secondary antibodies were from Santa Cruz (Santa Cruz, CA). An XTT cell proliferation assay kit was obtained from Trevigen (Gaithersburg, MD). VECTASHIELD hard set mounting medium with 4,6-diamidino-2-phenylindole (DAPI) was purchased from Vector Laboratories (Burlingame, CA). Recombinant human tumor necrosis factor alpha (TNFα) was purchased from Millipore (Temecula, CA). 2', 7'-dihydrodichlorofluorescein diacetate, doxorubicin, paclitaxel, methotrexate, fenretinide and 4-hydroxy tamoxifen were from EMD Biosciences (San Diego, CA). Gemcitabine was a gift from Dr. Yixing Jiang. D-*threo*-1-phenyl-2-decanoylamino-3-morpholino-1-propanol (PDMP) was purchased from Biomol (Plymouth Meeting, PA). All other lipids were from Avanti Polar Lipids (Alabaster, AL). All other reagents were purchased from Sigma (St. Louis, MO).

Cell culture. Human SH-SY5Y neuroblastoma cells, human U-87 MG glioblastoma cells and human LN-18 glioblastoma cells were grown in DMEM medium supplemented with 10% fetal bovine serum, 100 U/ml penicillin and 100 U/ml streptomycin (humidified atmosphere, 5% CO_2, 37°C) in 100 mm tissue culture dishes (Falcon). For subculture, cells were washed with PBS (phosphate buffer saline) then treated with 0.5 mg/ml trypsin and 0.2 mg/ml EDTA (5–15 min), resuspended and centrifuged (200x g_{max}, 2 min) and plated in 100 mm tissue culture dishes (2 x 10^7 cells per dish), 6-well tissue culture plates (5 x 10^6 cells per well) or 96-well tissue culture plates (5 x 10^3 to 5 x 10^4 cells per well).

Liposome preparation and cellular transfection. Aliquots of lipids were made at appropriate ratios (**Table 1**), and dried to a film under a stream of nitrogen, then hydrated by addition of 0.9% NaCl to a final lipid concentration of 25 mg/ml. Solutions were sealed, heated at 60°C (60 min) and subjected to vortex mixing and sonicated until light no longer diffracted through the suspension. The lipid vesicle-containing solution was quickly extruded at 60°C by passing the solution 10 times through 100 nm polycarbonate filters in an Avanti Mini-Extruder (Avanti Polar Lipids, Alabaster, AL). Nanoliposome solutions were stored at 4°C until use, protected from light when necessary. To prepare siRNA- or plasmid-loaded cationic nanoliposomes, siRNA or plasmid DNA, was aliquoted into 0.9% NaCl and nanoliposomes were added in a 10:1 weight ratio to nucleic acid. The solution was allowed to incubate overnight at room temperature prior to use. The RNA interference sequences utilized (**Table 2**), were from the ON-TARGET plus SMART pool product line of Dharmacon (Lafayette, CO).

Liposome size determination. Liposome suspensions were diluted 1:10 in 0.9% NaCl prior to size determination. Light scattering was used to quantify the size of liposomes using a Malvern Instruments Zetasizer Nano (Malvern, Worcestershire, United Kingdom).

Glucosylceramide synthase construct generation. Glucosylceramide synthase cDNA (Gene, UGCG; Accession, BC038711) was transferred by PCR sub-cloning into the mammalian expression vector pcDNA3.1 (Invitrogen, Carlsbad, CA). The construct was sequence-verified by the Molecular Genetics Core Facility at the Pennsylvania State University College of Medicine.

Plasma membrane translocation of $p67^{phox}$. Plasma membrane proteins were prepared by biotinylation and streptavidin affinity purification as previously described.[19] SH-SY5Y cells grown in 6-well plates for transfected with siRNA or plasmid (200 nM or 3 μg/ml, respectively, 48 h) or preincubated with arachidonyl trifluoromethyl ketone (ATK, 10 μM, 60 min) or C8-glucosylceramide (10 μM, 60 min), prior to TNFα stimulation (100 ng/ml, 15 min). Next, cultures were washed with HBSS pH 7.5 containing 0.1 g/l $CaCl_2$ and 0.1 g/l $MgCl_2$ (HBSS-CM), incubated with 0.5 mg/ml sulfo-NHS-biotin (20 mM HEPES in HBSS-CM pH 8.0, 40 min, on ice) and excess sulfo-NHS-biotin was neutralized with 50 mM glycine (HBSS-CM, on ice, 15 min). Cells were scraped into HBSS-CM, centrifuged (200x g_{max}, 2 min), lysed in 500 μL loading buffer (20 mM HEPES in HBSS pH 7.5, 1% Triton X-100, 0.2 mg/ml saponin, 1% PIC) and after brief sonication, incubated with streptavidin-agarose beads (25 μl, 2 h, 4°C). Beads were collected by centrifugation (2,500x g_{max}, 2 min) and re-suspended in 150 μl of loading buffer (5 min, boiling water bath) to release bound protein. Supernatants were obtained by centrifugation (2,500x g_{max}, 2 min) and analyzed by western blotting.

Quantification of reactive oxygen species production. SH-SY5Y, U-87 MG or LN-18 cells were seeded in 96-well tissue culture dishes (5 x 10^4 cells per well) and grown for 48 hours. Cultures were incubated with 50 μM of the oxidation-sensitive fluorescent indicator 2', 7'-dihydrodichlorofluorescein diacetate (H_2DCFDA) for one hour in the presence or absence of pharmacological inhibitors, N-acetyl-L-cysteine (5 mM) or C8-glucosylceramide (10 μM). Alternatively, cells were transfected with siRNA (200 nM) or plasmid (3 μg/ml), 48 h prior to exposure, the last hour of which included H_2DCFDA loading. H_2DCFDA is de-acetylated in the cytosol to dihydrodichlorofluorescein and increases in fluorescence upon oxidation by H_2O_2 to dichlorofluorescein (DCF). Following exposure to stimuli, cultures were washed with PBS, agitated in lysis buffer (2 M Tris-Cl pH 8.0, 2% w/v SDS, 1 mM Na_3VO_4) and total DCF fluorescence intensity was quantified in 100 μl of cell lysates using a Beckman Coulter Multimode DTX 880 microplate reader (Fullerton, CA) with a 495 nm excitation filter and a 525 emission filter. All DCF fluorescence data were normalized to the average DCF fluorescence under control conditions (relative DCF-fluorescence values).

Glucosylceramide synthase activity. Generation of fluorescent NBD-glucosylceramide was quantified as follows. Samples of whole cell lysates containing 5 μg of total protein (BCA protein assay) were reacted with 100 μM NBD-ceramide in 5 mM $MnCl_2$

Table 1. Nanoliposome formulations

Formulation	Lipids	Molar ratio
Cationic	DOTAP:PEG2000-DSPE:DOPE	4.75:0.5:4.75
Ghost	DSPC:DOPE:PEG2000-DSPE	5.66:2.87:1.47
Ceramide	DSPC:DOPE:PEG2000-DSPE: PEG750-C8CER:C6CER	3.75:1.75:0.75: 0.75:3
Ceramide + PDMP	DSPC:DOPE:PEG2000-DSPE: PEG750-C8CER:C6CER:PDMP	3.75:1.75:0.75: 0.75:1.5: 1.5
Basic	DSPC:DOPC:DOPE:PS:SM:CH	0.8:0.8:1:0.4:1: 4
BasicCer	DSPC:DOPC:DOPE:PS: SM:CH:C8CER	0.8:0.8:1: 0.4:1:4:1
BasicGluCer	DSPC:DOPC:DOPE:PS:SM: CH:GLUCER	0.8:0.8:1: 0.4:1:4:1
BasicCerGluCer	DSPC:DOPC:DOPE:PS:SM: CH:C8CER:GLUCER	0.8:0.8:1: 0.4:1:4:1:1

Liposome formulations were prepared from specific lipids, at particular molar ratios, prior to nano-sizing. 1,2-dioleoyl-*sn*-glycero-3-phosphocholine (DOPC), 1,2-distearoyl-*sn*-glycero-3-phosphocholine (DSPC), 1,2-dioleoyl-*sn*-glycero-3-phosphoethanolamine (DOPE), 1,2-distearoyl-*sn*-glycero-3-phosphoethanolamine-N-(methoxy[polyethylene glycol]-2000) (PEG2000-DSPE), 1,2-dioctanoyl-*sn*-glycero-3-phospho-L-serine (PS), 1,2-dioleoyl-3-trimethylammonium-propane (DOTAP), C6-ceramide (C6CER), C8-ceramide (C8CER), C8-ceramide-1-succinyl[methoxy(polyethylene glycol)-750] (PEG750-C8CER), C8-glucosylceramide (GLUCER), C18-sphingomyelin (SM), cholesterol (CH), and D-threo-1-phenyl-2-decanoylamino-3-morpholino-1-propanol (PDMP).

Table 2. Target sequences for siRNA

ID #	Target sequence
J-006441-05	GCG AAU CCA UGA CAA UAU A
J-006441-06	GGA CCA AAC UAC GAA UUA A
J-006441-07	GAU CCU AAC UUA AUC AAC A
J-006441-08	GGA AUG UCU UGU UUA AUG A

ON-TARGET plus SMART pool siRNA was obtained from Dharmacon (Lafayette, CO). Four separate sequences within the human glucosylceramide synthase gene (Gene, UGCG; Accession, BC038711) were targeted.

pH 7.2, 30 μg/ml BSA and 1 mM UDP-glucose (100 μl reaction volume, 60 min, 37°C). After termination of the reaction (100 μl dichloromethane), lipids were extracted (Bligh-Dyer) and separated by thin layer chromatography (chloroform/acetone/methanol/acetic acid/water at 10:4:3:2:1). NBD-glucosylceramide was quantified using a GE Healthcare Typhoon Imager (Piscataway, NJ) running ImageQuant software.

Superoxide dismutase activity. Interference of ferrictyochdrome reduction by superoxide was measured as an indication of superoxide dismutase (SOD) activity. Samples of whole cell lysates containing 5 μg of total protein (BCA protein assay) were added to a solution of 50 μM hypoxanthine, 6 nM xanthine oxidase, 100 μM EDTA and 10 μM ferricytochrome c in a 50 mM potassium phosphate pH 7.8 (100 μl reaction volume, 30 min, 25°C) and ferricytochrome reduction was quantified using a Beckman Coulter Multimode DTX 880 microplate reader (Fullerton, CA), reading absorbance at 550 nm.

Catalase activity. Interference of horseradish peroxidase-mediated formation of the fluorescent resorufin from Amplex Red was quantified as an indication of catalase activity. Samples of whole cell lysates containing 5 μg of total protein (BCA protein assay) were mixed with 0.1 M Tris-Cl pH 7.4 and 10 mM $MgCl_2$ (volume of 75 μl) prior to incubation with 10 μM H_2O_2 (25 μl) for 30 min at 37°C. Next, an equal volume (100 μl) of horseradish peroxidase (2 U/ml) and Amplex Red (100 μM) was added to the reaction mixture and resorufin fluorescence was quantified using a Beckman Coulter Multimode DTX 880 microplate reader (Fullerton, CA), with a 530 nm excitation filter and a 590 emission filter.

Cellular viability assay. SH-SY5Y, U-87 MG or LN-18 cells were seeded in 96-well tissue culture dishes (5 x 10^3 cells per well) and grown for 48 hours. Cultures were co-incubated with pharmacological inhibitors and either 100 ng/ml TNFα or 5 μg/ml doxorubicin, for 48 hours. Alternatively, cells were transfected with siRNA (200 nM) or plasmid (3 μg/ml), 48 hours prior to TNFα or doxorubicin exposure. XTT reagent prepared according to the manufacturer (Trevigen, Gaithersburg, MD) was added and allowed to incubate for 4 hours. Viability was determined by absorbance at 490 nm (650 nm ref.), using a Beckman Coulter Multimode DTX 880 microplate reader (Fullerton, CA). All values were normalized to the average values under control conditions.

Statistical analysis. One-way or two-way, analysis of variance (ANOVA), were used to determine statistically significant differences between treatments ($p < 0.05$). At least three independent experiments were performed for each condition. Post hoc comparisons of specific treatments were performed using a Bonferroni test. Unpaired t-tests were used to directly compare mean diameters of respective liposome formulations. All error bars represent standard error from the mean (SEM). All statistical analyses were carried out using GraphPad Prism 4 software (La Jolla, CA).

Acknowledgements

We would like to thank Keystone Nano, Inc., (State College, PA) and in particular Amy Knupp and Dr. Mylisa Parette, for the use of and assistance with, the Malvern Zetasizer Nano instrument. We graciously thank Dr. Yixing Jiang, of the Milton S. Hershey Penn State Medical Center, for kindly providing gemcitabine. Discussions with Dr. Marvin Schulte, Dr. Barbara Taylor and Dr. Kristin O'Brien, of the University of Alaska-Fairbanks, were helpful during the preparation of this manuscript. This research was funded in part by USDA grant 2005-34495-16519 (T.B.K.), NIH grant U54 NS41069 (T.B.K.) and NIGMS grant GM77391 (M.C.C.). Additional financial support was made possible by the College of Natural Sciences and Mathematics, University of Alaska-Fairbanks.

References

1. Andrieu-Abadie N, Gouaze V, Salvayre R, Levade T. Ceramide in apoptosis signaling: Relationship with oxidative stress. Free Radic Biol Med 2001; 31:717-28.
2. Ogretmen B, Hannun YA. Biologically active sphingolipids in cancer pathogenesis and treatment. Nat Rev Cancer 2004; 4:604-16.
3. Zheng W, Kollmeyer J, Symolon H, Momin A, Munter E, Wang E, et al. Ceramides and other bioactive sphingolipid backbones in health and disease: Lipidomic analysis, metabolism and roles in membrane structure, dynamics, signaling and autophagy. Biochim Biophys Acta 2006; 1758:1864-84.
4. Bedard K, Krause KH. The NOX family of ROS-generating NADPH oxidases: Physiology and pathophysiology. Physiol Rev 2007; 87:245-313.
5. Cacicedo JM, Benjachareowong S, Chou E, Ruderman NB, Ido Y. Palmitate-induced apoptosis in cultured bovine retinal pericytes: Roles of NAD(P)H oxidase, oxidant stress and ceramide. Diabetes 2005; 54:1838-45.
6. Hannun YA. Functions of ceramide in coordinating cellular responses to stress. Science 1996; 274:1855-9.
7. Senchenkov A, Litvak DA, Cabot MC. Targeting ceramide metabolism—a strategy for overcoming drug resistance. J Natl Cancer Inst 2001; 93:347-57.
8. Lambeth JD, Kawahara T, Diebold B. Regulation of nox and duox enzymatic activity and expression. Free Radic Biol Med 2007; 43:319-31.
9. Lambeth JD. Nox/Duox family of nicotinamide adenine dinucleotide (phosphate) oxidases. Curr Opin Hematol 2002; 9:11-7.
10. Graham KA, Kulawiec M, Owens KM, Li X, Desouki MM, Chandra D, et al. NADPH oxidase 4 is an oncoprotein localized to mitochondria. Cancer Biol Ther 2010; 10: 223-31.
11. Wang R, Dashwood WM, Nian H, Lohr CV, Fischer KA, Tsuchiya N, et al. NADPH oxidase overexpression in human colon cancers and rat colon tumors induced by 2-amino-1-methyl-6-phenylimidazo[4,5-b]pyridine (PhIP). Int J Cancer 2010; In press.
12. Naughton R, Quiney C, Turner SD, Cotter TG. Bcr-abl-mediated redox regulation of the PI3K/AKT pathway. Leukemia 2009; 23:1432-40.
13. Richards SM, Clark EA. BCR-induced superoxide negatively regulates B-cell proliferation and T-cell-independent type 2 ab responses. Eur J Immunol 2009; 39:3395-403.
14. Belda-Iniesta C, de Castro Carpeno J, Casado Saenz E, Cejas Guerrero P, Perona R, Gonzalez Baron M. Molecular biology of malignant gliomas. Clin Transl Oncol 2006; 8:635-41.
15. Smith PS, Zhao W, Spitz DR, Robbins ME. Inhibiting catalase activity sensitizes 36B10 rat glioma cells to oxidative stress. Free Radic Biol Med 2007; 42:787-97.
16. Gouaze-Andersson V, Cabot MC. Glycosphingolipids and drug resistance. Biochim Biophys Acta 2006; 1758:2096-103.
17. Liu YY, Han TY, Giuliano AE, Cabot MC. Ceramide glycosylation potentiates cellular multidrug resistance. FASEB J 2001; 15:719-30.
18. Liel Y, Rudich A, Nagauker-Shriker O, Yermiyahu T, Levy R. Monocyte dysfunction in patients with gaucher disease: Evidence for interference of glucocerebroside with superoxide generation. Blood 1994; 83:2646-53.
19. Barth BM, Stewart-Smeets S, Kuhn TB. Proinflammatory cytokines provoke oxidative damage to actin in neuronal cells mediated by Rac1 and NADPH oxidase. Mol Cell Neurosci 2009; 41:274-85.
20. Ozben T. Oxidative stress and apoptosis: Impact on cancer therapy. J Pharm Sci 2007; 96:2181-96.
21. Wang J, Yi J. Cancer cell killing via ROS: To increase or decrease, that is the question. Cancer Biol Ther 2008; 7:1875-84.
22. Wang H, Maurer BJ, Reynolds CP, Cabot MC. N-(4-hydroxyphenyl) retinamide elevates ceramide in neuroblastoma cell lines by coordinate activation of serine palmitoyltransferase and ceramide synthase. Cancer Res 2001; 61:5102-5.
23. Wang H, Maurer BJ, Liu YY, Wang E, Allegood JC, Kelly S, et al. N-(4-hydroxyphenyl)retinamide increases dihydroceramide and synergizes with dimethylsphingosine to enhance cancer cell killing. Mol Cancer Ther 2008; 7:2967-76.
24. Stover TC, Sharma A, Robertson GP, Kester M. Systemic delivery of liposomal short-chain ceramide limits solid tumor growth in murine models of breast adenocarcinoma. Clin Cancer Res 2005; 11:3465-74.
25. Tran MA, Smith CD, Kester M, Robertson GP. Combining nanoliposomal ceramide with sorafenib synergistically inhibits melanoma and breast cancer cell survival to decrease tumor development. Clin Cancer Res 2008; 14:3571-81.
26. Zolnik BS, Stern ST, Kaiser JM, Heakal Y, Clogston JD, Kester M, McNeil SE. Rapid distribution of liposomal short-chain ceramide in vitro and in vivo. Drug Metab Dispos 2008; 36:1709-15.
27. Tran MA, Gowda R, Sharma A, Park EJ, Adair J, Kester M, et al. Targeting V600EB-raf and Akt3 using nanoliposomal-small interfering RNA inhibits cutaneous melanocytic lesion development. Cancer Res 2008; 68:7638-49.
28. Kline CL, Shanmugavelandy SS, Kester M, Irby RB. Delivery of PAR-4 plasmid in vivo via nanoliposomes sensitizes colon tumor cells subcutaneously implanted into nude mice to 5-FU. Cancer Biol Ther 2009; 8:1831-7.
29. Matters GL, Harms JF, McGovern CO, Jayakumar C, Crepin K, Smith ZP, et al. Growth of human pancreatic cancer is inhibited by downregulation of gastrin gene expression. Pancreas 2009; 38:151-61.
30. van Meer G, Voelker DR, Feigenson GW. Membrane lipids: Where they are and how they behave. Nat Rev Mol Cell Biol 2008; 9:112-24.
31. Ueyama T, Tatsuno T, Kawasaki T, Tsujibe S, Shirai Y, Sumimoto H, et al. A regulated adaptor function of $p40^{phox}$: Distinct $p67^{phox}$ membrane targeting by $p40^{phox}$ and by $p47^{phox}$. Mol Biol Cell 2007; 18:441-54.
32. Hannun YA, Luberto C. Ceramide in the eukaryotic stress response. Trends Cell Biol 2000; 10:73-80.
33. Hannun YA, Obeid LM. Principles of bioactive lipid signalling: Lessons from sphingolipids. Nat Rev Mol Cell Biol 2008; 9:139-50.
34. Moskwa P, Palicz A, Paclet MH, Dagher MC, Erdos M, Marodi L, et al. Glucocerebroside inhibits NADPH oxidase activation in cell-free system. Biochim Biophys Acta 2004; 1688:197-203.
35. Farokhzad OC, Langer R. Impact of nanotechnology on drug delivery. ACS Nano 2009; 3:16-20.
36. Castel V, Grau E, Noguera R, Martinez F. Molecular biology of neuroblastoma. Clin Transl Oncol 2007; 9:478-83.
37. Block ML, Zecca L, Hong JS. Microglia-mediated neurotoxicity: Uncovering the molecular mechanisms. Nat Rev Neurosci 2007; 8:57-69.
38. Farooqui AA, Horrocks LA, Farooqui T. Modulation of inflammation in brain: A matter of fat. J Neurochem 2007; 101:577-99.